Rock and Soil Mechanics

Volume 44 | Issue 7 Article 4

11-3-2023

Investigation of the fracture process zone and behavior of the macro-scale fatigue cracks in brittle rock specimens

Nazife ERARSLAN

Civil Engineering Department, Izmir Demokrasi University, 35140, Turkey; School of Civil Engineering, The University of Queensland, 4072, Australia (Guest lecturer)

Recommended Citation

ERARSLAN, Nazife (2023) "Investigation of the fracture process zone and behavior of the macro-scale fatigue cracks in brittle rock specimens," *Rock and Soil Mechanics*: Vol. 44: Iss. 7, Article 4.
DOI: 10.16285/j.rsm.2022.00244
Available at: https://rocksoilmech.researchcommons.org/journal/vol44/iss7/4

Investigation of the fracture process zone and behavior of the macro-scale fatigue cracks in brittle rock specimens

Abstract

The importance of this study is to explain the fatigue damage mechanism while addressing the effect of fatigue on the fracture toughness (KIC) using the brittle Brazilian specimens and to show for the first time in the literature the behavior of macroscale cracks that open and close in brittle rock without leading to eventual failure. The KIC was reduced by 35% due to the cyclic loading, and the reduction of the indirect Brazilian strength was found to be reduced by 30%. The fatigue cracks were observed to open and close elastically without failure and have been recorded by a camera for hours in brittle rock specimens with sinusoidal loading for the first time in the rock mechanics field in this study. The findings of the scanning electron microscope (SEM) and computed tomography (CT) revealed that the failure of the Brazilian disc and chevron crack notched Brazilian disc (CCNBD) specimens was caused by the formation of the fracture process zone (FPZ), which included many microcracks rather than a single macrocrack propagation during the cyclic loading tests. Moreover, SEM and CT findings indicated the FPZ took place ahead of the kerf crack tip, leading to the visible fatigue crack opening and closing elastically in brittle rock specimens without any rupture. According to the experimental and numerical analysis results, the FPZmax could be obtained with the 60º inclined notch crack. This demonstrates the maximum FPZ development possible with combined mode I-II (tensile and shear) loading.

Keywords

CCNBD rock specimens, rock fatigue, FPZ and rock fatigue

Rock and Soil Mechanics 2023 44(7): 2041−2049 ISSN 1000−7598
https: //doi.org/10.16285/j.rsm.2022.00244 http://rocksoilmech.researchcommons.org/journal

Investigation of the fracture process zone and behavior of the macro-scale fatigue cracks in brittle rock specimens

ERARSLAN Nazife[1, 2]

1. Civil Engineering Department, Izmir Demokrasi University, 35140, Turkey

2. School of Civil Engineering, The University of Queensland, 4072, Australia (Guest lecturer)

Abstract: The importance of this study is to explain the fatigue damage mechanism while addressing the effect of fatigue on the fracture toughness (K_{IC}) using the brittle Brazilian specimens and to show for the first time in the literature the behavior of macroscale cracks that open and close in brittle rock without leading to eventual failure. The K_{IC} was reduced by 35% due to the cyclic loading, and the reduction of the indirect Brazilian strength was found to be reduced by 30%. The fatigue cracks were observed to open and close elastically without failure and have been recorded by a camera for hours in brittle rock specimens with sinusoidal loading for the first time in the rock mechanics field in this study. The findings of the scanning electron microscope (SEM) and computed tomography (CT) revealed that the failure of the Brazilian disc and chevron crack notched Brazilian disc (CCNBD) specimens was caused by the formation of the fracture process zone (FPZ), which included many microcracks rather than a single macrocrack propagation during the cyclic loading tests. Moreover, SEM and CT findings indicated the FPZ took place ahead of the kerf crack tip, leading to the visible fatigue crack opening and closing elastically in brittle rock specimens without any rupture. According to the experimental and numerical analysis results, the FPZ_{max} could be obtained with the 60^{o} inclined notch crack. This demonstrates the maximum FPZ development possible with combined mode I-II (tensile and shear) loading.

Keywords: CCNBD rock specimens, rock fatigue, FPZ and rock fatigue

1 Introduction

When a new stress-induced crack develops in a material under any load, the stress state in the material is greatly affected. The reorganized stress state in the material causes the cracks in the brittle rock material to propagate, blunt or change direction, which greatly affects the strength of the material[1]. Griffith[2] was the first to explain the importance of the effect of pre-existing cracks and newly formed micro-level cracks on the strength of the material. He argued that all brittle materials contain small pre-existent cracks, and these cracks will create newly formed cracks, and failure occurs when all these cracks coalesce. Griffith's theory marked a turning point in the history of fracture mechanics research, despite the limitation that these crack formations can only occur in the plane of existing cracks.

Linear elastic fracture mechanics (LEFM) principles state that cracks are able to grow when the stress condition at the tip of a crack exceeds the strength value of the material. The geometry of a crack and the axis of the acting load strongly influence the stress distribution at the crack tip, and the stress condition is expressed by three general fracture states according to the LEFM. A crack can propagate in three modes: Mode I (tensile stress), Mode II (shear stress), and Mode III (tear stress). The fracture mode in a material is considered one of these three states, depending on the geometry and value of the crack surface displacement[3]. In the case of a Mode I fracture, an opening is expected on the crack surface starting from the crack tip. In Mode II, in-plane slippage is expected at the crack surfaces. Finally, in Mode III, the crack surfaces move perpendicular to the crack axis due to the out-of-plane shear stress.

In general, mixed-mode I-II fracturing occurs with compressive stress and is much more complicated than those with tensile stress. The tensile cracks initiate and propagate depending on the direction of induced maximum principal stress[4−7]. The stress density factor around a crack tip under tensile loading and the LEFM principles that apply to stress calculations are also used for stress calculations at a crack tip under compression loading. K_I (mode I stress intensity factor) indicates the level of stress intensity acting at the crack tip, while a negative K_{II} (mode II stress intensity factor) indicates shear stress acting parallel to the crack plane in the opposite direction.

Brittle materials are able to be failed with lower load amounts due to cyclic loading and fatigue effect[8−10]. This occurs due to the 'fatigue' failure of any material. Metro tunnel walls, dams, excavation roofs, bridges, and road foundations are a few examples that can be attenuated by cyclic/repetitive loading. In general, rock fatigue research in literature establishes a relationship between the reduction

Received: 2 September 2022 Accepted: 21 February 2023
Corresponding author: NAZİFE Erarslan, female, born in 1977, PhD, Associate Professor, research interests: rock mechanics, fracture mechanics, and soil mechanics. E-mail: nazife.dogan@idu.edu.tr

of applied maximum stress (S) and the number of cycles (N)[9, 11−13]. However, not much concern has been given to researching the deformation mechanism of rock fatigue[14−15]. In damage mechanics research, horizontal and vertical deformation/strain values are generally investigated. However, these values are result of the formation and propagation of micro/nano cracks. Therefore, research will be more accurate if they are made with parameters related to the mechanism that causes the values used. Therefore, one of these parameters was studied in this article: fracture toughness value. The mean of fracture toughness (K_{IC}) parameter is the resistance of a material against crack initiation. Erarslan[15] found that the K_{IC} values determined under cyclic loading were lower than those under monotonic stress. Erarslan[16] found that the K_{IC} value found with cyclic tests is 34% lower than the K_{IC} value found with static tests. This is a significant decrease in strength and in this case, it clearly shows that the fracture resistance of cracks in rocks is reduced by cyclic loads. It can be concluded that the strength values obtained by monotonic loading in engineering structures should not be ultimate and that damage and failure may occur at lower loads due to cyclic loads.

The stress-induced crack initiation in some materials, such as concrete and rocks, usually leads to stable crack growth first, and plastic deformation occurs around the tip of these cracks due to the bridging effect. This zone is called the fracture process zone (FPZ) (Fig. 1). The FPZ at the tip of a notch crack is divided into two zones, (i) Inner zone: preliminary crack development; and (ii) Outer zone: unsteady crack development. In the inner zone, the stresses induced in the specimens ascend faster than the increment of crack propagation and this causes linear deformation[17−18]. It is substantial to indicate that a small crack growth takes place due to the microcrack formation leading to strain hardening around the crack tip zone. This zone keeps developing till the stress concentration reaches a crucial value, K_{IC}, which is fracture toughness due to the plastic deformation developed within this zone. In the outer zone, the induced stress within the specimen decreases more slowly with a higher displacement due to the development of unsteady cracks.

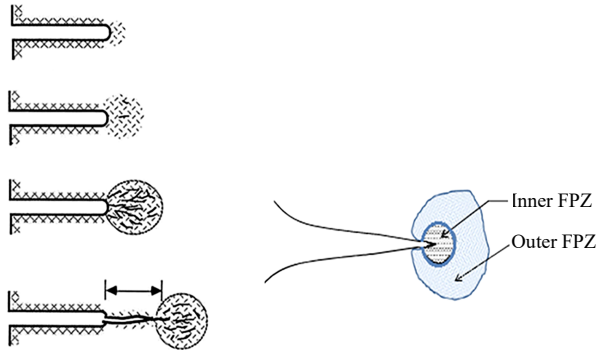

(a) Development of FPZ (b) Two FPZ zones at the tip of a crack

Fig. 1 Fracture process zone

In some studies, it is proposed that the FPZ region at the crack tip must be formed previously for crack growth or the FPZ region may form behind the tip instead of the crack tip (Fig. 2)[19−22]. Observation of the FPZ region is not easy besides using numerical analysis and some imaging techniques. There are some studies in the literature that the FPZ was observed and analyzed by using scanning electron microscope (SEM) and computing tomography (CT) techniques[21, 23].

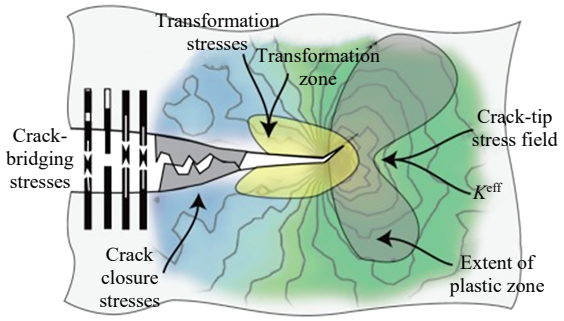

Fig. 2 FPZ and bridging behind the crack tip (Withers[24])

2 Experimental & numerical studies

In this research, the Brazilian disc test and the fracture toughness test, which are recommended by the International Society of Rock Mechanics (ISRM) standards, have been carried out[19]. Both experiments were done in five replicates for the static and repetitive loading tests. The Brazilian disc tests were done using the rock specimens obtained from the tuff-type rocks.

The specimens have 123 MPa uniaxial compressive strength (UCS). The diameter of the Brazilian discs test specimens was 51 mm. The CCNBD specimen geometry, which is one of the suggested ISRM standards, was preferred to use with the static and repetitive tests. The CCNBD sample contains a kerf crack within the geometry, and it makes the CCNBD appropriate for all fracturing mode loading. Some of the untested Brazilian disc and CCNBD specimens are given in Fig. 3. The important specimen geometries are the notches thickness (t) and the specimen thickness (B) and the radius of specimen (R). These values are 1.4 mm and 26.0 mm respectively. The kerf crack parameters are the length of the inner kerf crack a_0, and the length of the outer kerf crack a_1. These values are 16−18 mm and 37 mm respectively (Fig. 3). Instron 2 670 model clip gauge was used to measure the crack mouth opening displacement (CMOD) (Fig. 3(c)). In Fig. 3, R is the radius of the specimen, and R_S is the distance

between the tip of the external crack and the center of the specimen.

(a) Some prepared Brazilian disc specimens (b) CCNBD specimens (c) CMOD recorder clip gauge

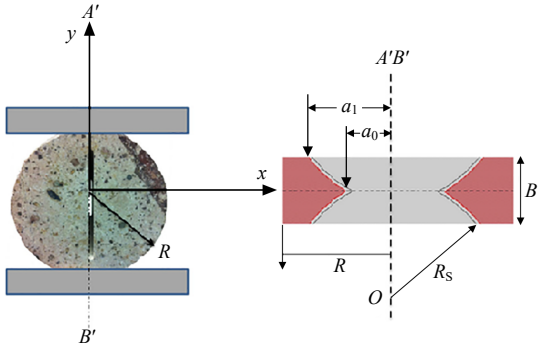

(d) CCNBD geometry between loading plates (e) CCNBD geometry parameters

Fig. 3 CCNBD specimen and its geometry parameters

The *S*–*N* curve, which was obtained with the sinusoidal repetitive tests, indicates the reduction of rock strength with the increasing number of load cycles (*N*) with the relative maximum stress (*S*). The easiest method to achieve the *S*–*N* curve in the fatigue tests is reducing the applied load until no failure occurs at each test. In general, the *S*–*N* curve approach was used with the uniaxial compressive loading tests using the cylindrical specimens[20–22]. Therefore, repetitive loading tests with diametrical indirect tensile stress in this study were performed for the first time. The frequency in the sinusoidal loading tests was 1 Hz. Cyclic loading tests with a constant mean level and constant amplitude, termed sinusoidal cyclic loading, were performed to obtain the *S*–*N* curve. The sinusoidal cyclic tests to obtain the *S*–*N* curve of a material were started at a high-stress level of ~2/3 of the tensile strength of the material. The applied force was then reduced by about 10% to the stress level at which the specimens no longer broke at lower stress levels, which is called the fatigue limit of the specimen. The numerical analysis series were done by using ABAQUS software with the heterogeneity description implemented with extended finite element method (XFEM) and Simpleware software. Computed tomography (CT) scanned images were prepared using an appropriate pixel threshold filter (image segmentation based on the pixel information by converting to a binary image) for post-image processing. The Mask data technique in Simpleware (based on voxel information) was employed to count the greyscale pixels to quantify the microfractures volume/area of the FPZ within the tested specimens. This reconstruction image is called binary coding, and it simply extracts heterogeneous image components for the construction of the meshing process of any XFEM numerical analysis.

3 Results of the experimental and numerical studies

The static Brazilian tensile strength of the samples was found to be 11 MPa by taking the average of five samples. On the other hand, the static mode I (tensile) fracture toughness value was found to be 1.48 MPa· $m^{\frac{1}{2}}$ by using five CCNBD specimens.

The fatigue tests were performed successfully under repetitive loading using both Brazilian and CCNBD rock specimens. The *S*–*N* plots of the Brazilian test and CCNBD tests are demonstrated in Fig. 4 respectively. The *S*–*N* plots indicated the strength of the CCNBD sample decreases with the increasing load amplitude. Moreover, the *S*–*N* plot results of the CCNBD tests showed that the final toughness strength of the specimens decreased by 35% (from 1.48 kN to 1.21 kN) due to the fatigue impact. Therefore, K_{IC} value was found reduced to be 30%. This impressive result shows that unstable cracking progress

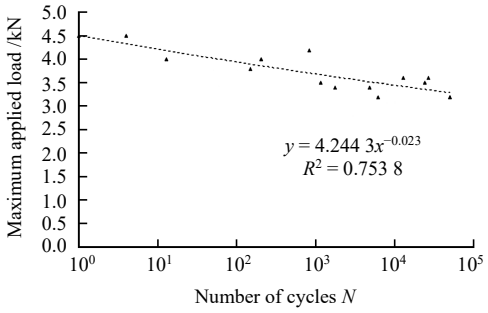

(a) The fracture toughness test

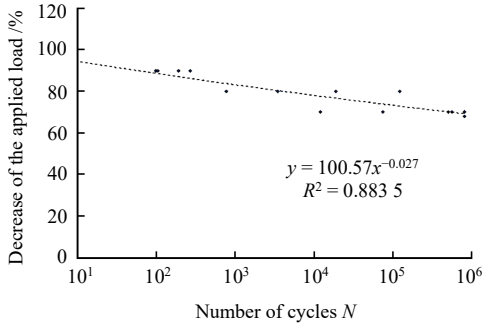

(b) The Brazilian tests

Fig. 4 *S*–*N* plots

is likely with below the stress values at the crack tip (K_I) than the K_{IC} determined under monotonic loading. This result contradicts the classical fracture mechanics theory because fracture mechanics principles indicate that crack growth is not probable as long as K_I is lower than K_{IC}. On the other hand, the Brazilian tensile strength of the specimens was found reduced up to 30% due to fatigue (Fig. 4(b)).

The results of CCNBD and Brazilian tensile test are shown in Tables 1 and 2.

Table 1 The sinosoidal cyclic loading test results of CCNBD specimens

Sample	Failure load /kN	# of cycles N	Fracture endurance (K_{IC}) /(MPa· $m^{\frac{1}{2}}$)
CCNBD-R1	1.28	4 776	0.72
CCNBD-R2	1.31	45 345	0.74
CCNBD-R3	1.20	48 689	0.70

Table 2 The sinosoidal repetitive loading test results of Brazilian specimens

Sample	Ultimate load /kN	# of cycles (N) up to failure	Brazilian tensile strength /MPa
BR-1	34.7	929 435	8.20
BR-2	33.8	987 456	7.98
BR-3	33.5	986 890	8.01

The synchronous recording of the fatigue crack opening and closing, quite critical part of this study, has been supplied in Video 1 (Annex 1). The brittle rocks fail abruptly after a small plastic deformation, which usually occurs after elastic deformation. The synchronous recording of the opening and closing of the crack, which acts like an elastic spring at the centre of the rock sample during the experiment, before failure makes this research impressive. In some studies, in the literature, crack formation is recorded by super-fast cameras, but the movement of a visible fatigue crack shown by this research is different from the studies in the literature. The crack formation and failure with the monotonic process shown in the previous studies occur abruptly. However, the macro fatigue crack was obtained open and close without final failure and recorded using a camera for hours. This is an impressive observation that is contrary to many fracture theories and the behaviour of brittle materials.

It is important to explain how cracks supplied with Annex 1 open and close elastically for hours without failure under repetitive loading. This may be possible to explain using the FPZ concept at the crack tip. This zone absorbs the energy required for the macro fatigue crack and behaves as a buffer at the tip of the kerf crack. At this point, the following question should be explained: Why does the existence of the FPZ not cause new macro crack initiations leading to failure? The details of this case are given in 'Discussion'. The pictures captured by the video supplied in the Annex 1 are shown in Fig. 5.

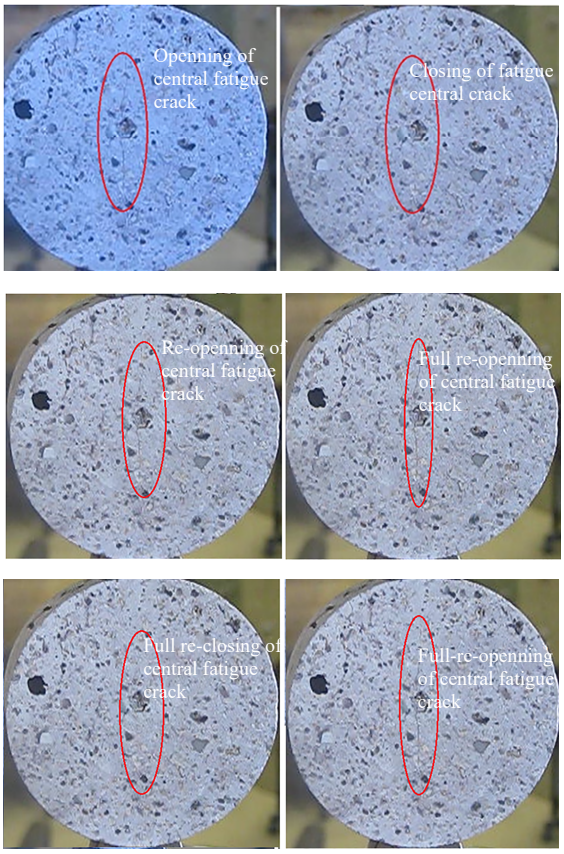

(a) For the Specimen 1

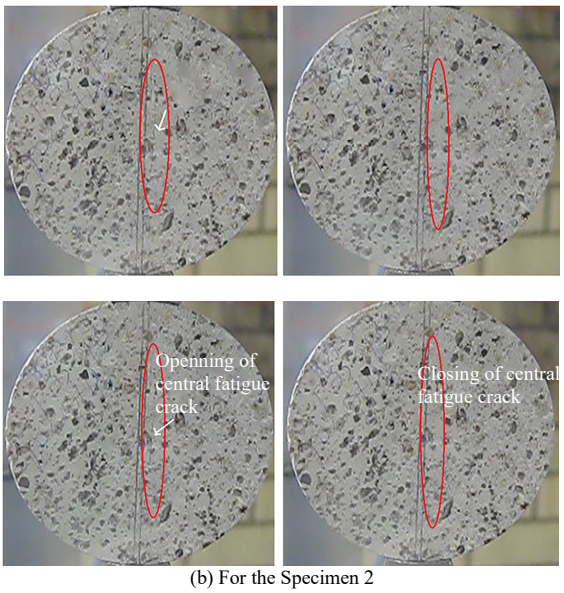

(b) For the Specimen 2

Fig. 5 The captured figures obtained from the video given in Annex 1

Some of the repetitive stress-CMOD plots of both CCNBD and Brazilian specimens are shown in Fig. 6. The most obvious result in the plots is the formation of high plastic deformation, and the accumulation of this

plastic deformation indicates the formation of the FPZ at the crack tip (Fig. 6(a)). The fatigue damage developed in the specimen is detected by a large amount of plastic deformation occurring without failure and can be seen from the stress-CMOD plots showing displacement along the x and y directions, as shown in Figure 6(b)−6(c). It can be seen from the graphs that both diametrical axial displacement and CMOD increase at different rates with damage increases. The CMOD deformation initially occurs with a little elastic deformation, followed by rapid plastic deformation and accumulation. On the other hand, a very interesting failure behaviour was obtained with the fatigue cracking caused by tensile stress in the Brazilian tests under repetitive loading. The opening of the central fatigue crack is observed with the increase of the CMOD data in positive values. The CMOD readings, however, describe crack opening due to accumulated plastic deformation up to about 60% of the experiment.

The obtained positive CMOD readings then turned into negative values, in which case it is concluded that the fatigue crack has begun to close. It was determined subsequently that the accumulation of plastic deformation, which continued with the closure of this crack, continued until the final fracture occurred. The obtained results are believed to guide future research on the fatigue of brittle materials.

The physical qualification of the FPZ was done by using SEM and X-ray with CT scanning in this study (Fig. 7). The FPZ and many micro and macro cracks in front of the notch crack were determined using the CT scan. The cracks in the FPZ are macro scale and start from the tip of the kerf crack, while the cracks close to the specimen boundary are considerably smaller. This result shows that macro crack formation starts at the tip of the kerf crack and the FPZ zone developed due to the large energy deposition at the tip of the kerf crack. This deposited energy reduction is due to the formation of new cracks. The decreasing energy was also modelled using XFEM numerical analyses and shown in Fig. 9. The damaged zone in front of the notch cracks on the other hand were investigated directly with the SEM analysis. It was believed that the preparation of thin section from the specimens causes extra microcracking

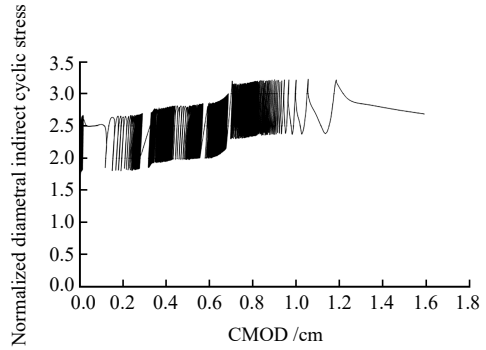

(a) The stress-CMOD graph of CCNBD specimens

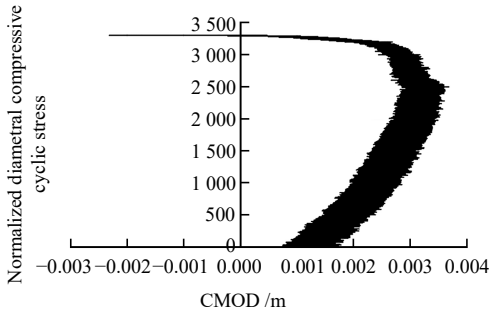

(b) Brazilian test of CCNBD specimens

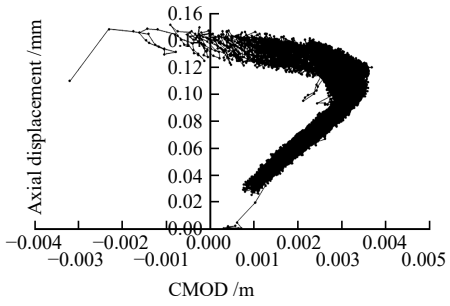

(c) The axial displacement-CMOD graph of CCNBD specimens

Fig. 6 The stress-CMOD graph Brazilian test and the axial displacement-CMOD graph of CCNBD specimens

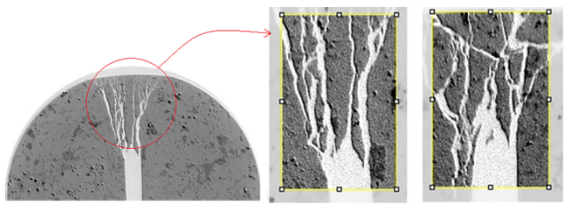

(a) CT images of failure surface within the CCNBD specimen (Ghamgosar et al.[22])

(b) SEM images of failure surface at 500 μm

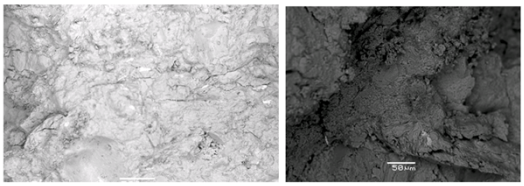

(c) SEM images of failure surface at 100 μm and 50 μm

Fig. 7 The formation of FPZ within CCNBD specimen

on the surface of the failed specimen. The CT scan and the SEM figures are shown in Fig. 8. The CCNBD specimens have an important advantage in the geometry allows to focus and investigation of the crack tip directly (Fig. 7). The rough topography of the failure surface with dust and small pieces indicates the development of FPZ at the tip.

The numerical analysis to investigate the primary stresses and fracture properties at the crack tips has been performed using XFEM-based programs (Fig. 8). The modeling of the static and repetitive loading was performed separately to investigate the fatigue effect at and around the notch cracks. The results of the XFEM modeling showed that the distribution of the tensile stress occurs in front of the kerf crack to develop a broad FPZ region with repetitive loading (Fig. 9(b)). In contrast, there is an influential tensile region just along the kerf crack axis rather than the tip with static loading. (Fig. 9(a)).

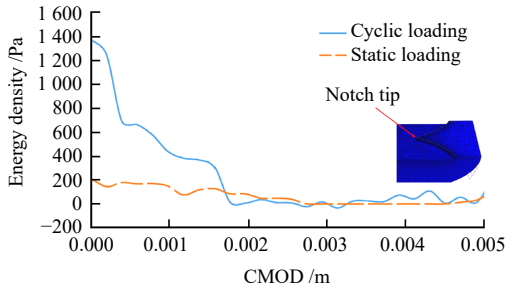

Fig. 8 The comparison of accumulated energy density between cyclic and static loading

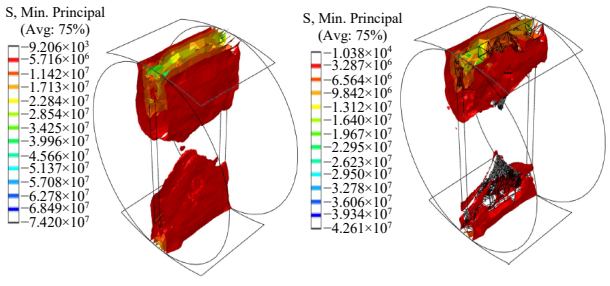

(a) With static loading (b) With periodic loading (Ghamgosar et al.[22])

Fig. 9 The stress condition at the crack tip and FPZ development

The energy accumulation at the tip of notch crack within the CCNBD specimen with the static loading was found lower compared to the recurrent loading (Fig. 9). The work done is more because more cracks and small particles are generated due to repetitive loading. Moreover, the accumulative energy discharges as it diverges from the crack tip. Hu et al.[25] found the similar results in literature.

4 Discussion

The development and the location of FPZ in ductile and brittle materials have been investigated by many researchers[18, 23, 26]. The generalized Dugdale model (GDM) (named cohesive crack model), one of the well-known fictitious or cohesive crack approaches is one of the most famous models used in the literature. The dimensions of the FPZ according to the Dugdale model do not change until the failure occurs with the constant crack closing stresses in the FPZ. On the other hand, the size of this zone is described in Barenblatt's model as smaller compared with the length of induced macro crack[18, 23, 26]. Moreover, the FPZ in front of the crack in brittle materials has been assumed as linear elastic until failure occurs[18, 23]. Therefore, the FPZ zone was analysed with SEM and CT scan in this study without these assumptions given in the literature. The numerical analysis and experimental results especially SEM images showed the heterogenous rock texture due to grains covered by a matrix and interlocked grains playing a very important role in the development of FPZ, plastic strain accumulation and fatigue damage mechanism of rocks. The results also showed that crack growing is possible with below stress than the determined static strength of the material. The load-strain plots in this study showed a huge amount of plastic strain accumulation due to the new stress-induced crack developments. This type of plastic strain accumulation without failure has been believed due to the 'subcritical crack phenomenon' in literature. Moreover, subcritical cracks induce failure with a lower failure load compared to the determined strength of the material. Thus, the fracture toughness value and the Brazilian tensile strength values were found reduced to be 30%−35%. This reduction may explain the pre-existing and/or induced stable sub-critical cracks are possible to be developed with lower loads compared with the static strength of the material. It means the crack propagation may occur with lower stress intensity factor (SIF) values (K_I) at the crack tip than the fracture toughness (K_{IC}) of a material. These results seem to contradict the fracture mechanics principles because the fracture mechanics principles state that crack propagation does not consist as long as K_I is lower than K_{IC}[3]. The sub-critical crack phenomenon has been believed in this study to be liable for the comprise of the FPZ and the deformation mechanism of rock fatigue. Moreover, this phenomenon is believed to be used for investigating the mechanism and failure of many materials due to the time- dependent loading such as creep and fatigue in many structures. Some experimental investigations are revealing that subcritical phenomena, which are characterized by the initiation and growing of a large

number of microcracks, have been observed even before the appearance of macro cracks[15−16, 25−26].

In this study, the presence of the FPZ region was directly demonstrated by using SEM and CT scan methods. However, the most important point to be discussed in this study is how the visible fatigue cracking in a brittle rock behaves elastically. It was previously stated that the development of the FPZ zone causes such a fatigue crack to open and close elastically. Then the following question should be discussed: Does this macro crack behave like an elastic material because of the occurrence of the FPZ or does the FPZ develop later due to the opening and closing action of this visible crack? This is a very difficult question to be explained. In the literature, it is stated that the FPZ region and the accumulative energy are required for the FPZ to act as a bridge between the damaged area and the undamaged area and for the commencing of fractional and macro cracks that lead to deformation. On the other hand, it is indicated in many studies that nano and microcracks in the FPZ region grow and then coalesce to form a visible crack[25, 29−34]. FPZ on the other hand in brittle materials such as ceramics and rocks, develops quite large including fractional and macro cracks with the remaining cohesive pressure in the FPZ[34−42]. It was concluded in this research after the detailed evaluation of the experimental and numerical analysis results that the pre-existent cracks in heterogeneous materials such as concrete, rock, and some composites are the causes of the FPZ zone developed under repetitive loading. The new stress-induced cracks then develop within the FPZ to initiate macro cracks leading to failure. Whittaker et al.[3] stated that macro crack is developed because of the traction-free region behind the crack tip and the FPZ at the tip. They proposed the undamaged bonds located behind the crack tip may cause the closing of the crack faces while the crack tends to grow and open further to overcome that closing force. The transition of the closing forces to the opening forces in front of the crack tip is believed in this research because of the local stress generated between grains and matrix, and the pre-existing microcracks. The size of maximum FPZ(FPZ_{max}) is found using following equations when $\sigma_1 = \sigma_t$ (where σ_1 is the maximum principal stress; σ_t is the maximum tensile stress)[22]:

$$r_{FPZ}(\theta)\left|_{\theta \neq 0} = \frac{1}{2\pi}\left(\frac{K_I}{\sigma_t}\right)^2 \cos^2\left(1+\left|\sin\frac{\pi}{2}\right|\right)^2\right| \quad (1)$$

where r_{FPZ} is the radius of FPZ; r_θ is the radius of the plastic fracture process zone; θ is notch crack inclination angle.

The maximum FPZ is then calculated by derivation of Eq. (2):

$$\mathrm{Max}(r_{FPZ})(\theta) = \frac{\left[2\cos\left(\frac{1}{2}\theta\right)^2 \sin\left(\frac{1}{2}\theta\right) + 3\cos\left(\frac{1}{2}\theta\right)^2 - 2\sin\left(\frac{1}{2}\theta\right) - 2\right]\cos\left(\frac{1}{2}\theta\right)K_{IC}^2}{2\sigma_t^2} \quad (2)$$

The maximum size of FPZ was found with the 60º inclined notch crack. It means the FPZ_{max} may develop when the fracturing mode is mixed mode I-II (tensile-shear). The presence of both the tensile and shear stresses within the FPZ are also able to be seen with the presence of dust and small particles in the SEM images given earlier and 3D graphics. Shear stress and rough surface peaks resulting from cracks can be seen in Fig. 10.

The features of rock fatigue have been explained in the literature that more fractional and subcritical cracks in FPZ are obtained compared to the static loading[42−48]. This result was also determined using both experimental and numerical modelling in this study. Fig. 11(a)−11(b) shows the physical differences on the failure surface between monotonic load and repetitive load. A damaged region with fractional particles and dust at the crack tip in the CCNBD specimen tested under repetitive loading was determined (Fig. 11(b)), whereas almost no dust and small particles were obtained in front of the crack tip in the CCNBD specimen failed under static loading (Fig. 11(a)). The similar results were obtained with the XFEM numerical analysis (Fig. 11(c)−11(d)). Therefore, investigation of the FPZ using the CCNBD specimen and chevron cracks is believed to be necessary and beneficial for investigating the fatigue mechanism of brittle materials.

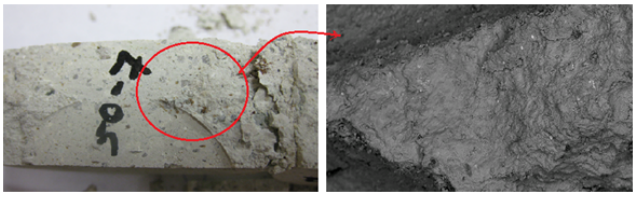

(a) Failure surface and the notch crack tip in the CCNBD specimen and the SEM image

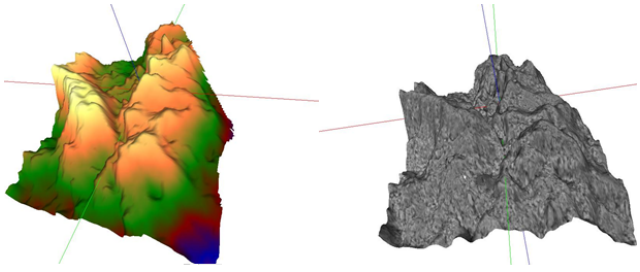

(b) 3D graphs of the 2D SEM image given in (a)

Fig. 10 The failure surface of the notch crack within the CCNBD

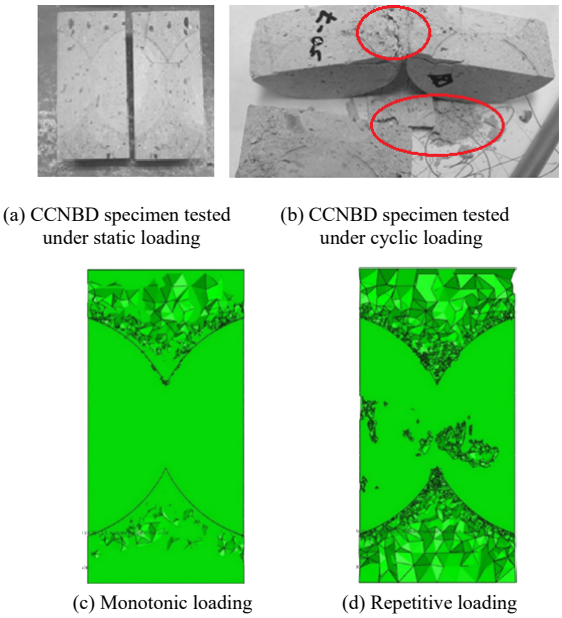

(a) CCNBD specimen tested under static loading (b) CCNBD specimen tested under cyclic loading

(c) Monotonic loading (d) Repetitive loading

Fig. 11 Tested CCNBD specimens under static and cyclic loading and their relative numerical modelling

5 Conclusions

The fracture toughness and indirect Brazilian tensile strength tests have been conducted with both static and repetitive loading in this study. The maximum reduction of the static K_{IC} was obtained to be 35% due to the repetitive loading and the maximum reduction of the indirect Brazilian strength was found to be 30% due to the repetitive loading. Both strength reductions were found as indications of the effect of fatigue on the tensile strength of rocks.

The permanent strain accumulation in front of the crack tip within CCNBD and Brazilian disc specimens tested under repetitive loading were obtained clearly to quantify the damage due to microfractures developed in the FPZ. The CT and SEM findings showed that the failure of Brazilian disc and CCNBD specimens failed under repetitive loading is due to the presence of FPZ including many fractional cracks, instead of a single macrocrack. A crushed region including much fractional particles in front of the kerf crack tip in the CCNBD specimen was obtained with the cyclic loading, whereas no fractional pieces were observed at the failure surface of specimens with the static loading tests. The FPZ_{max} was found only with the 60° inclined notch crack. The reason of the transition between the closing forces and the opening forces in front of the crack tip is believed in this research because of the local stress generated between the grains, matrix, and the pre-existent microcracks. As a result, the opening and closing of a visible fatigue crack behave elastically without leading to failure in brittle rocks and have been recorded using a video camera for hours for the first time in the rock mechanics area with this study.

Declaration of competing interest

The author declares that they have no known competing financial interests or personal relationships that could have appeared to influence the work reported in this paper.

Acknowledgments

Acknowledgement is made to the Geotechnical Engineering Centre at The University of Queensland, Australia.

Annex. Supplementary data

The following are the Supplementary data to this article:

http://ytlx.whrsm.ac.cn/fileup/1000-7598/SUPPL/20230717092021.mp4

References

[1] BRACE W F, BOMBOLAKIS E G. A note on brittle crack growth in compression[J]. Journal of Geophysics and Research, 1963, 68: 30709−3713.

[2] GRIFFITH A A. The phenomena of rupture and flow in solids[J]. Philosophical Transactions of the Royal Society A: Mathematical, Physical and Engineering Sciences, The Royal Society, 1920, 221: 163−198.

[3] WHITTAKER B N, SINGH R N, SUN G. Rock fracture mechanics—principles, design and applications[M]. Amsterdam: Elsevier, 1992.

[4] AL-SHAYEA N A. Crack propagation trajectories for rocks under mixed-mode I–II fracture[J]. Engineering Geology, 2005, 81: 84−97.

[5] LING L B. Effect of cyclic fatigue loading on matrix multiple fracture of fiber-reinforced ceramic-matrix composites[J]. Ceramics, 2019, 2(2): 345−353.

[6] HOEK E. Brittle fracture of rocks[M]. London: John Wiley, 1968: 99−124.

[7] LI Y P, CHEN L Z, WANG Y H. Experimental research on pre-cracked marble under compression[J]. International Journal of Solids and Structures, 2005, 42: 2505−2516.

[8] BURDINE N T. Rock failure under dynamic loading conditions[J]. SPE Journal, 1963(3): 1−8.

[9] ATTAWEL P B, FARMER I W. Fatigue behavior of rock[J]. International Journal of Rock Mechanics and Mining Science, 1973, 10: 1−9.

[10] EVANS A G, FULLER E R. Crack propagation in ceramic materials under cyclic loading conditions[J]. Metallurgical Transactions, 1974, 5: 27−29.

[11] TAO Z, MO H. An experimental study and analysis of the behaviour of rock under cyclic loading[J]. International Journal of Rock Mechanics and Mining Science, 1990, 27: 5−15.

[12] BAGDE M N, PEDROS V. Fatigue properties of intact sandstone samples subjected to dynamic uniaxial cyclical loading[J]. International Journal of Rock Mechanics and Mining Science, 2005, 42: 237−250.

[13] HAIMSON B C. Effect of cyclic loading on rock[J]. Dynamic Geotechnical Testing, 1978, 654: 228−245.

[14] LAVROV A. Kaiser effect observation in brittle rock cyclically loaded with different loading rates[J]. Mechanics of Materials, 2001, 33: 669−677.

[15] ERARSLAN N. Microstructural investigation of subcritical crack propagation and fracture process zone (FPZ) by the reduction of rock fracture toughness under cyclic loading[J]. Engineering Geology, 2016, 208: 181−190.

[16] ERARSLAN N, WILLIAMS D W. Investigating the effect of fatigue on fracturing resistance of rocks[J]. Journal of Civil Engineering and Architecture, 2012, 6(10): 1310.

[17] ATKINSON B K. Subcritical crack growth in geological materials[J]. Journal of Geophysics and Research, 1984, 89: 4077−4114.

[18] BARENBLATT G I. The mathematical theory of equilibrium cracks in brittle fracture[J]. Advanced Applications Mechanics, 1962, 7: 55−129.

[19] ISRM. Suggested method for determining mode I fracture toughness using cracked chevron notched Brazilian disk (CCNBD) specimens[J]. International Journal of Rock Mechanics and Mining Sciences, 1995, 32(1): 57−64.

[20] FAN J, CHEN L, JIANG D Y. Fatigue properties of rock salt subjected to interval cyclic pressure[J]. International Journal of Fatigue, 2016, 90: 109−115.

[21] GATELIER N, PELLET F, LORET B. Mechanical damage of an anisotropic porous rock in cyclic triaxial tests[J]. International Journal of Rock Mechanics and Mining Sciences, 2002, 39: 335−354.

[22] GHAMGOSAR M, ERARSLAN N. Experimental and numerical studies on development of fracture process zone (FPZ) in rocks under cyclic and static loading[J]. Rock Mechanics and Rock Engineering, 2016, 49(3): 893−908.

[23] DUGDALE D.S. Yielding of steel sheets containing slits[J]. Journal of Mechanics and Physics of Solids, 1960, 8: 100−104.

[24] WITHERS P J. Fracture mechanics by three-dimensional crack-tip synchrotron X-ray microscopy[J]. Philosophical Transactions of Series A, Mathematical, Physical, and Engineering Sciences, 2015, 373(3): 2036.

[25] HU X, DUAN K. Influence of fracture process zone height on fracture energy of concrete[J]. Cement Concrete Research, 2004, 34: 1321−1330.

[26] HILLERBORG A. Analysis of one single crack[M]. [S. l.]: Elsevier, 1983: 223−250.

[27] ORTEGA A P, MIAMI E V, GONZALES D T. Characterization of the translaminar fracture cohesive law[J]. Composites Part A: Applied Science and Manufacturing, 2016, 91(2): 501−509.

[28] KO T Y, KEMENY J. Determination of the subcritical crack growth parameters in rocks using the constant stress-rate test[J]. International Journal of Rock Mechanics and Mining Sciences, 2013, 59: 166−178.

[29] BAZANT Z P, CEDOLIN L. Blunt crack band propagation in finite element analysis[J]. Journal of Engineering Mechanics, 1979, 105: 297−315.

[30] CARLSSON J, ISAKSSON P. Crack dynamics and crack tip shielding in a material containing pores analysed by a phase field method[J]. Engineering Fracture Mechanics, 2019, 206: 526−554.

[31] RITCHIE R O. Mechanisms of fatigue crack propagation in metals, ceramics, and composites: role of crack tip shielding[J]. Material Science and Engineering A, 1988, 103(1): 15−28.

[32] SALIBA A, LOUKILI A, GREGORIE D, Experimental analysis of crack evolution in concrete by the acoustic emission technique[J]. Frattura ed Integrità Strutturale, 2015, 34: 300−308.

[33] LABUZ J F, CATTANEO S, CHEN L. Acoustic emission at failure in quasi-brittle materials[J]. Construction and Building, Materials, 2001, 15: 225−233.

[34] RILEM TC212-ACD recommendation. Acoustic emission and related NDE techniques for crack detection and damage evaluation in concrete[S]. [S. l.]: Materials and Structures, 2010.

[35] LABUZ J F, SHAH S P, DOWDING C H. The fracture process zone in granite: evidence and effect[J]. International Journal of Rock Mechanics and Geomechanics Abstract, 1987, 24(4): 235−246.

[36] RITCHIE R O. Mechanisms of fatigue-crack propagation in ductile and brittle solids[J]. International Journal of Fracture, 1999. 100, 55−83.

[37] WITHERS P J. 3D crack-tip microscopy: illuminating micro-scale effects on crack-tip behaviour[J]. Advanced Engineering Materials, 2011, 13: 1096−1100.

[38] COLLIN F. Cyclic and fatigue behaviour of rock materials: review, interpretation and research perspectives[J]. Rock Mechanics and Rock Engineering 2017, 51: 391−414.

[39] LAJTAI E Z. A theoretical and experimental evaluation of the Griffith theory of brittle fracture[J]. Tectonophysics, 1971, 11: 129−156.

[40] HALLBAUER D K, WAGNER H, COOK N G V. Some observations concerning the microscopic and mechanical behaviour of quartzite specimens in triaxial compression tests[J]. International Journal of Rock Mechanics and Mining Sciences, 1973. 10: 713−726.

[41] ZANG A, WAGNER C, STANTHITCHS T, et al. Fracture process zone in granite[J]. Journal of Geophysical Research, 2000, 105(B10): 23651−23661.

[42] ZHU P, YOUNG L, LI Z. The shielding effects of the crack-tip plastic zone[J]. International Journal of Fracture, 2010, 161(2): 131−139.

[43] COSTIN L S, HOLCOMB D J. Time-dependent failure of rock under cyclic loading[J]. Tectonophysics, 1981, 79(3−4): 279−296.

[44] HADLEY K. The effect of cyclic stress on dilatancy: another look[J]. Journal of Geophysical Research, 1976. 81(14): 2471−2474.

[45] TAPPONNIER P, BRACE W F. Development of stress-induced microcracks in Westerly granite[J]. International Journal of Rock Mechanics and Mining Sciences, 1976, 13: 103−112.

[46] HAIMSON B C, KIM C M. Mechanical behaviour of rock under cyclic fatigue[J]. Rock Mechanics, 1971(3): 845−863.

[47] SCHMIDT R G, LUTZ T J. K_{IC} and J_{IC} of Westerly granite-effects of thickness and in-plane dimensions[J]. Fracture Mechanics and Application of Brittle Materials, 1979, 678: 166−182.

[48] SINGH S K. Fatigue and strain hardening behaviour of greywacke from the flagstaff formation[J]. Engineering Geology, 1989, 26: 171−179.